Analysis of Lightning Surge Phenomenon and Surge Arrester Performance of a 400kV Transmission System

MD. SALAH UDDIN YUSUF, ABDUL MUNEM SAAD, MONIRA ISLAM, and CHOWDHURY AZIMUL HAQUE
Department of Electrical and Electronic Engineering
Khulna University of Engineering & Technology
Khulna- 9203
BANGLADESH
ymdsalahu2@gmail.com munemsaad@yahoo.com, monira_kuet08@yahoo.com, and c.azimulhaque@gmail.com

Abstract: - Lightning causes abrupt interruption in electrical power network. In this study a 400kV transmission system has been modelled to observe the influence of lightning surge current front time and tail time, back flashover phenomenon and performance of transmission line surge arresters. At first, induced voltage on the top of the tower has been observed for different front times and tail times of the same surge current function. A dynamic insulator flashover simulation model is also developed based on the voltage–time characteristics curve of the insulator string to observe the insulator flashover phenomenon. Effect of front time of the surge current on insulator flashover has been observed for the mentioned two different cases such as direct strike on the overhead ground wire and tower top of different surge currents and it has been found that insulator flashover phenomenon takes less time to occur for lower front times. Simulation results also show that although flashover occurred across the insulators placed on two horizontal ends of the transmission tower for lightning strike on the overhead ground wire and top of the tower, no flashover has occurred across the insulator placed on the horizontal midpoint of the tower. To implement transmission line surge arresters IEEE, Pinceti and Farnandez-Diaz surge arrester models were compared and the one with the better accuracy has been applied to observe the effectiveness of surge arresters against lightning surges. Three different cases containing different surge currents such as direct strike on the overhead ground wire, tower top and phase conductor have been taken into account for the surge arrester performance analysis. The induced overvoltage on the phase conductors with and without surge arresters has been analyzed for each cases using ATP Draw. In first two cases the induced voltage on the phase conductors are greater than the Basic Impulse Level (BIL). In case of direct strike on the phase, induced voltage is greater than BIL where the lightning strikes. Applying surge arresters has effectively reduced the induced voltage below the BIL thus preventing line outages in each case and it has been observed that for greater induced voltage arrester's percentage overvoltage suppression becomes higher.

Key-Words: - Lightning surge, Transmission Tower model, Flashover, Surge Arrester, ATP/EMTP.

1 Introduction

Lightning surge is a very natural and most unpredictable phenomenon which may disrupt power system and cause equipment's failure. Lightning generally strikes on the tall structure in everywhere. Because of the structural height transmission towers and lines are prone to lightning strike. Lightning can strike the overhead ground wire, tower top and phase a conductor which in turn causes extensive damage to the phase conductors and insulator strings by inducing overvoltage on phase conductors and across insulator strings. Flashover is also observed when voltages across the insulators become higher than the insulator withstands level and it causes serious damage to the system.

EMTP (Electro Magnetic Transient Program), NEC (Numerical Electromagnetic Calculation) and FDTD (Finite Difference Time Domain) methods are generally used for power system transient analysis. Among these EMTP or ATP (Alternating Transient Program) has gained more popularity because of its user-friendly environment. Transmission tower modelling is required to study the lightning transient behavior of a transmission tower. M. Ishii et al proposed a tower modelling approach using parallel RL circuits in [1]. In [2], T. Hara implemented a simple distributed line to represent the equivalent circuit of a transmission tower. Lightning phenomenon on a transmission tower was studied using NEC method representing the tower as an equivalent circuit following T.Hara

tower model [2] in [3]. In [4], M.Ishii's proposed equivalent circuit of transmission tower [1] was adopted to express a 132kV transmission tower for EMTP analysis. In [5], for a 77KV transmission tower a comparison between tower models in [1] and [2] was conducted. Representing the tower as a loss-less Constant-Parameter Distributed Line, back flashover event was observed across insulator strings when lightning strikes the overhead ground wire and phase conductor in [6]. In [7], transmission tower was expressed in M. Ishii's proposed equivalent circuit [1] to analyze the performance of line surge arresters using EMTP-RV software. It was stated that direct strike on the overhead ground wire or top of the tower will induce voltage on the phase conductors and across insulator string and induced voltage on the phase conductors and across insulators was later investigated for back flashover using PSCAD in [8].

Surge Arresters do not operate under normal voltage and provide a low impedance path to ground for a surge wave when lightning strikes. Thus surge arresters exhibit a non-linear behavior. In recent days, metal oxide or ZnO surge arresters have garnered more attention for surge protection. According to [9] ZnO surge arrester cannot be represented only by a non-linear resistance since its residual voltage is highly influenced by the magnitude and rate of rise of the surge current and an equivalent model to represent ZnO arrester was also proposed by IEEE Working Group in [9]. Another model was suggested by Pinceti based on the preceding model in [10]. Based on the IEEE model a simple and effective surge arrester model was presented by Farnandez-Diaz in [11]. In [6] Surge arrester was represented by the equivalent model presented in [10]. Surge arresters were implemented to the power system using Pinceti model [10] in [7]. Transmission line surge arresters were represented according to [9] in [12]. A comparative study between the surge arrester models has been conducted for a 132kV transmission system concluding that the Farnandez-Diaz model is more accurate in [13]. In this paper effect of surge front time and tail time during lightning surge event and performance of surge arresters for a 400kV transmission system have been studied.

The rest of the papers are organized as follows. Section 2 describes the transmission tower system with different parameters. Simulation results have been discussed in section 3. Finally section 4 concludes the result.

2 Transmission System Modelling

2.1 Transmission Line Model

400kV transmission tower with two overhead ground wires are considered for this study. The wires are 300km long. ACSR AFL-8 was taken as phase conductors with a resistance of 0.0557 Ω per kilometer [14] and AFL-1, 7 as the overhead ground wires conductors with a resistance of 0.417 Ω per kilometer [15]. In ATP Draw phase wires and ground wire are modeled separately using LCC template. For simplicity one transmission tower along with two tower spans has been considered. Line termination at each side is carried out by terminating the phase conductors with AC operation voltages and grounding the overhead earth wires to avoid any reflection that might affect the simulated high-voltages around the point of impact following [16].

2.2 Transmission Tower Model

In this study M. Ishii's proposed tower modelling method has been applied which is shown in Fig. 1, to model the 400 kV transmission tower presented in Fig. 2 [17]. Tower surge impedance Z is calculated from CIGRE recommended equation [18]:

$$Z = 60 \ln[\cot\{0.5 \tan^{-1}(\frac{R}{h})\}] \ (\Omega) \quad (1)$$

Where, the equivalent radius of the tower R can be determined with the help of Fig. 3a using the following equation:

$$R = \frac{r_1 h_2 + r_2(h_1+h_2) + r_3 h_1}{(h_1+h_2)} \ (m) \quad (2)$$

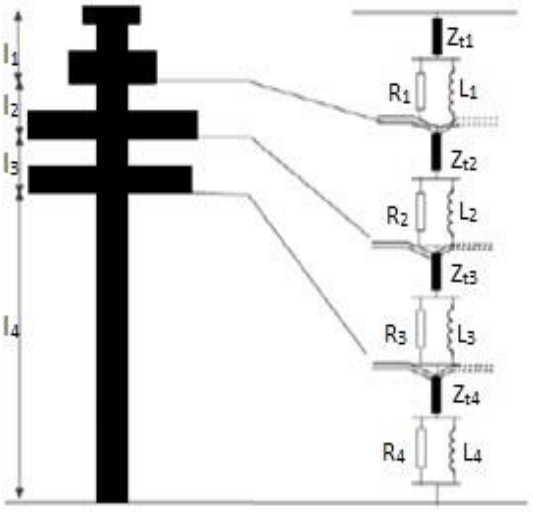

Fig. 1. Multistory tower model.

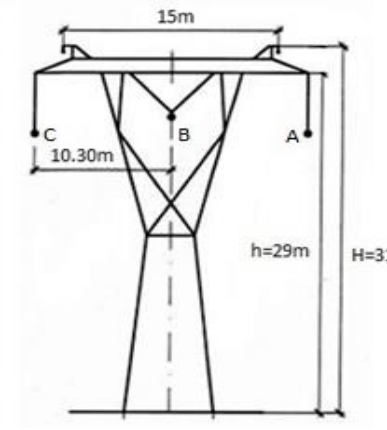

Fig. 2. 400kV transmission tower [17].

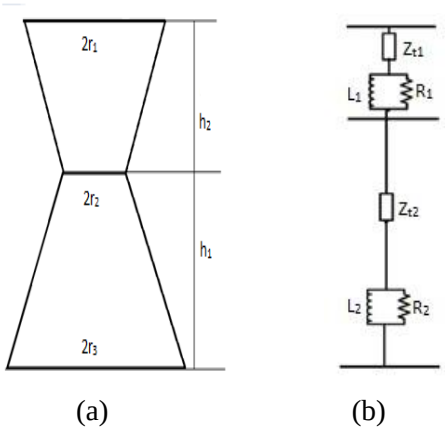

Fig. 3. Equivalent tower model.

Fig. 3b shows the equivalent circuit to represent the tower. The tower modelling equivalent parameters have been calculated from the following equations [5]:

$$Z_{t1} = 1.19Z \ (\Omega) \quad (3)$$
$$Z_{t2} = 0.81Z \ (\Omega) \quad (4)$$
$$\gamma = 0.8944 \quad (5)$$
$$\tau = \frac{2H}{v} \ (\mu s) \quad (6)$$
$$R_{t1} = -(2 \times Z_{t1} \times \ln \gamma) \ (\Omega) \quad (7)$$
$$R_{t2} = -(2 \times Z_{t2} \times \ln \gamma) \ (\Omega) \quad (8)$$
$$L_1 = R_{t1} \times \tau \ (\mu H) \quad (9)$$
$$L_2 = R_{t2} \times \tau \ (\mu H) \quad (10)$$

Where, Z_{t1} = surge impedance of the upper section of the tower, Z_{t2} = surge impedance of the lower section of the tower, R_{t1}= resistance of the R-L branch of the upper section of the tower, R_{t2}= resistance of the R-L branch of the lower section of the tower, L_1 = inductance of the R-L branch of the upper section of the tower, L_2= inductance of the R- L branch of the lower section of the tower, γ = attenuation co-efficient, τ = tower travel time, v = surge velocity and H= height of the tower.

2.3 Cross Arms Model

Cross arms are modelled as distributed constant lines following [2] and the surge impedance Z is given by:

$$Z = 60 \ln(\frac{2h}{r}) \ (\Omega) \quad (11)$$

Where, h = height of the cross arm, r = radius of the cross arm.

2.4 Insulator and Back Flashover Model

Insulator strings are represented as capacitor having equivalent capacitance value of 80pF per unit [19].

The withstand capability and back flashover mechanism of the insulator string can be expressed as following [19]:

$$V_{fo} = K_1 + \frac{K_2}{t^{0.75}} \ (kV) \quad (12)$$

Where, V_{fo}=flashover voltage,K_1 = *400*L*, K_2 *=710*L*, L = insulator length (meter), t =elapsed time after lightning stroke (μs).

If voltage between the terminals of the insulator becomes equal or greater than the flashover voltage from Equation (12), flashover will appear across the insulator string. Hence the insulator flashover event simulation model has been developed using a time dependent voltage controlled switch across the insulator strings following the flow diagram in Fig. 4. During simulation period both the voltage across the insulator is measured and the flashover voltage from Equation (12) is calculated simultaneously at an interval of Δt, which is actually the sampling time of the simulation. At any time instant, these two voltages are compared and if the voltage across the insulator string is equal or greater than the flashover voltage, the switch is closed to simulate the flashover event at the corresponding time instant.

2.5 Surge Arrester Model

In present days, Metal Oxide surge arresters gained more popularity for surge protection of transmission system. These arresters have high resistance under normal operating condition but show low resistance when system overvoltage occurs. According to [20] for a 400kV transmission system surge arrester of 336kV rated voltage is selected.

To represent the nonlinear behavior of surge arresters several models have been proposed. IEEE [9] and Pinceti [10] and Farnandez-Diaz [11] models have been chosen for comparison in this study.

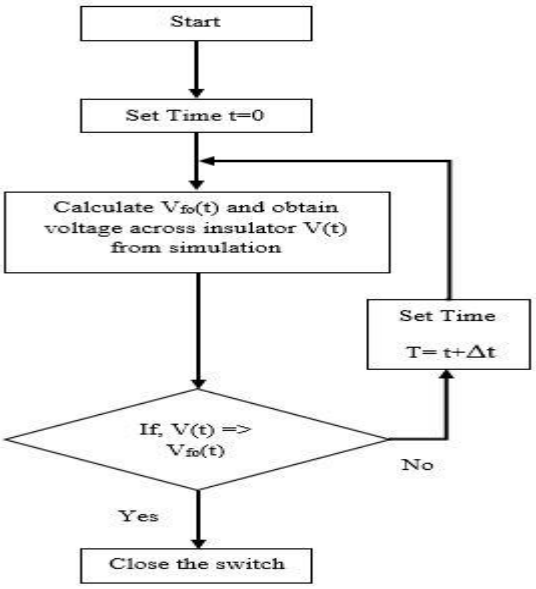

Fig. 4. Flashover simulation model flow diagram.

In IEEE model which is shown in Fig.5, the non-linear characteristics can be achieved using two arresters separated by an R-L filter. For slow-front surges the impedance of the filter is very low and the two non-linear arresters are practically in parallel. For fast-front surges R-L filter exhibits significant impedance resulting more current through A_0. Inductance associated with magnetic fields near the arrester is denoted by L_0. R_0 is placed to stabilize numerical integration in simulation software. Capacitance between the terminals of the arrester is denoted by C. The parameters are given as follows [9]:

$$L_1 = 15\frac{d}{n}\ (\mu H) \tag{13}$$

$$R_1 = 65\frac{d}{n}\ (\Omega) \tag{14}$$

$$L_0 = 0.2\frac{d}{n}\ (\mu H) \tag{15}$$

$$R_0 = 100\frac{d}{n}\ (\Omega) \tag{16}$$

$$C = 100\frac{n}{d}\ (pF) \tag{17}$$

Where, d= estimated height of the arrester, n= number of parallel columns of metal oxide in the arrester.

Fig. 6 shows Pinceti model which has some minor differences from IEEE model. The capacitance between the terminals is eliminated due to its negligible effect. Instead of two parallel resistors with the inductors a resistance of about 1MΩ is placed between the input terminals. The operating principle is quite similar to that of the IEEE model. The parameters can be determined from the following equations [10]:

$$L_1 = \frac{1}{4}\frac{V_{r\frac{1}{T_2}} - V_{r\frac{8}{20}}}{V_{r\frac{8}{20}}} V_n\ (\mu H) \tag{18}$$

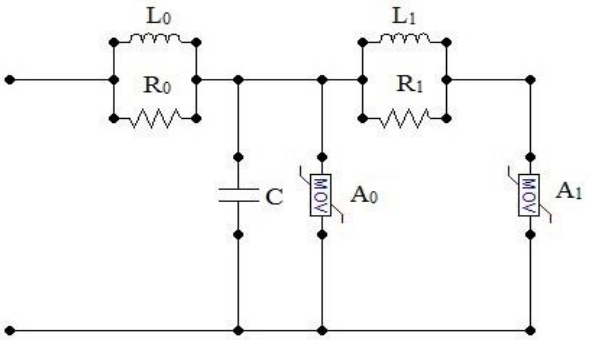

Fig. 5. IEEE model.

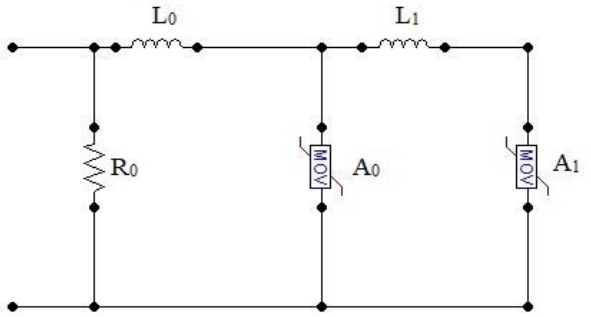

Fig. 6. Pinceti model.

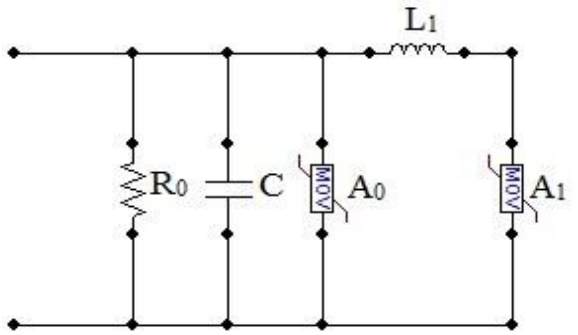

Fig. 7. Farnandez-Diaz model.

$$L_0 = \frac{1}{12}\frac{V_{r\frac{1}{T_2}} - V_{r\frac{8}{20}}}{V_{r\frac{8}{20}}} V_n\ (\mu H) \tag{19}$$

Where, V_n= Rated voltage of the arrester, $V_{r8/20}$ = Residual voltage for a (8/20) 10 kA lightning current and $V_{r1/T2}$ = Residual voltage for a (1/T2) 10 kA lightning current.

In Farnandez-Diaz model depicted in Fig. 7, only inductance between two non-linear branches is considered. Terminal to terminal capacitance has been taken into account. Like the Pinceti model, a resistance of about 1MΩ is connected across the input terminals. Parameters have been calculated from the following [11]:

$$L = \frac{1}{5}\frac{V_{r\frac{1}{20}} - V_{r\frac{30}{60}}}{V_{r\frac{8}{20}}} V_n\ (\mu H) \tag{20}$$

$$C = \frac{1}{55}\frac{V_{r\frac{1}{20}} - V_{r\frac{30}{60}}}{V_{r\frac{8}{20}}} V_n\ (pF) \tag{21}$$

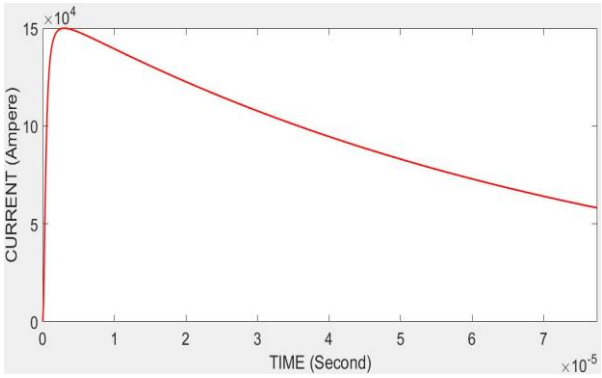

(a)

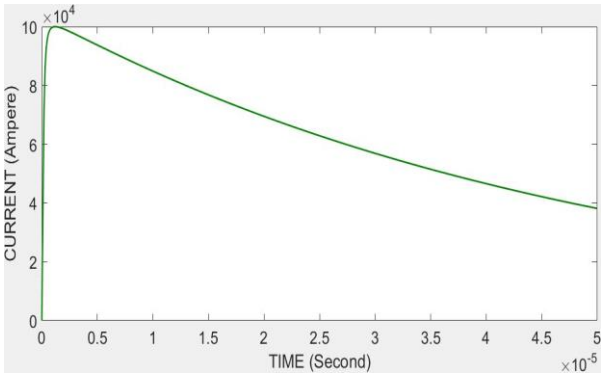

(b)

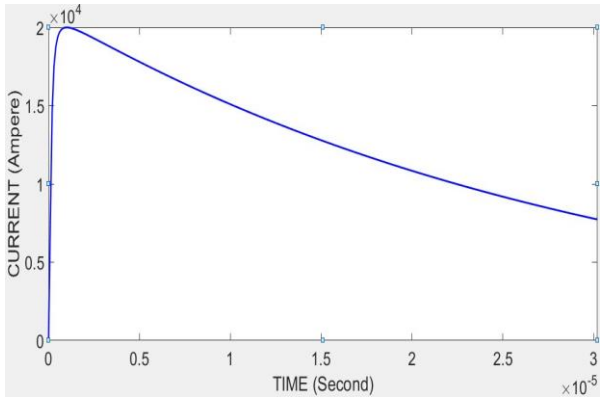

(c)

Fig. 8. Surge Current Waveforms.

Where, V_n = Rated voltage of the arrester, $V_{r8/20}$ = Residual voltage for a (8/20) 10 kA lightning current, $V_{r1/20}$ = Residual voltage for a (1/20) 10 kA lightning current and $V_{r30/60}$ = Residual voltage for a (30/60) 1 kA lightning current.

2.6 Lightning Model

Lightning current source can be expressed as Single Exponential function, Ramp type function, Double exponential function and Hiedler function. For simulation purposes Hiedler function [21] has been more popular in recent EMTP studies and so it has been selected in this study.

$$i(t) = I_0 \frac{(\frac{t}{\tau_1})^2}{(\frac{t}{\tau_1})^2+1} . e^{-t/\tau_2} \ (A) \quad (22)$$

Where, $i(t)$= instantaneous lightning current, I_0= peak value of lightning current, τ_1= front time of lightning current, τ_2=tail time of lightning current.

For back flashover studies crest value of the current source can be as high as 200kA [19]. Fig. 8a shows the surge current 150 kA (3/77.5 μs) that has been selected for direct strike on the overhead ground wire in this study following [6]. According to [8] 100kA (1.2/50 μs) and according to [4] 20kA (1/30.2 μs) have been selected for direct lightning surge on top of the tower and phase A conductor respectively and shown in Fig. 8b and Fig. 8c.The lightning strike is modeled by a Hiedler current source and a parallel lightning-path impedance of 400Ω.

3 Simulation and Result

3.1 ATP Draw model

Simulation has been carried out in ATP Draw software. The ATP Draw equivalent circuit of the transmission system is presented in Fig. 9. The values of the parameters are calculated from the preceding modelling scheme. The value of the tower footing resistance is considered to be 10 ohms as such was done in [4]. Length of the insulator strings is considered to be 4.3m [22].

3.2 Observations of Different Effect

3.2.1 Effect of Front time and Tail time

For lighting strike on an overhead ground wire, the front time of the lightning surge current has an influence on the induced voltage on top of the tower. Considering the peak amplitude of the surge current to be 150kA, the induced voltage wave shapes for different front times have been depicted in Fig. 10 which clearly shows that for a lower front time the induced voltage will be higher. For the front time of 1.2μs, 4μs and 6μs the induced voltage on the tower top is 7.8 MV, 7.5 MV and 7.2 MV respectively.

The same analysis has been carried out for tail time 20μs, 40μs and 60μs which is depicted in Fig. 11. It is apparent from the obtained voltage wave shapes that variation of maximum induced voltage for the same surge current with different tail times is negligible.

3.2.2 Effect of Surge Front Time on Insulator Flashover

Considering the first case scenario which is lightning strike on the overhead ground wire with 150kA surge current of a fixed tail time. For

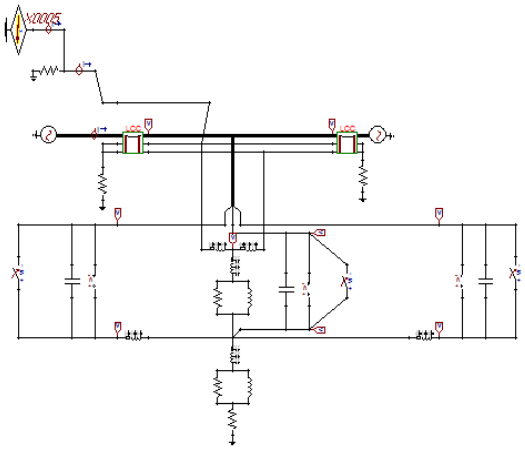

Fig. 9. Equivalent system model in ATP Draw.

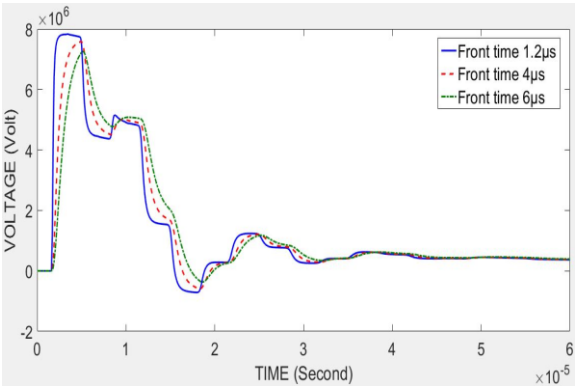

Fig. 10. Induced voltage on tower top for different front times.

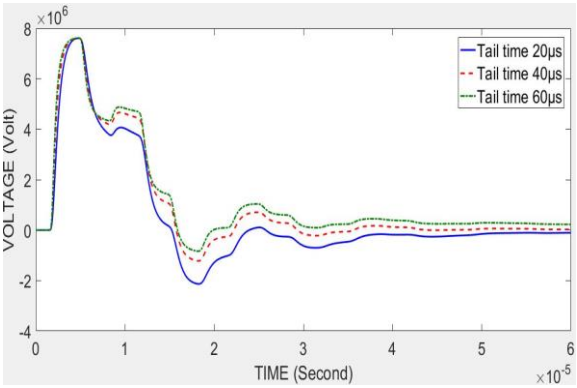

Fig. 11. Induced voltage on tower top for different tail times.

different front times of 1.2μs, 3μs, 5μs and 10μs of the surge current function voltage wave shapes across the insulators have been observed which are depicted in Fig. 12 and Fig. 13 respectively for insulators holding phase A and phase C. Table 1 presents a better understanding by providing the variation of time to insulator flashover occurrence with the variation of front time. It appears that voltage shapes across the insulators are highly influenced by the front time of surge current and lower front time causes faster flashover occurrence.

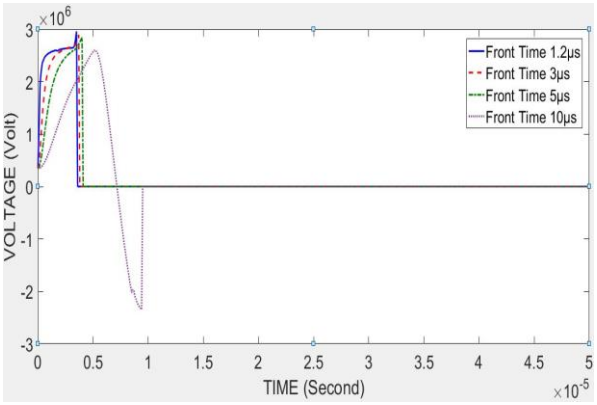

Fig. 12. Voltage across insulator holding phase A due to direct strike on overhead ground wire for different front times.

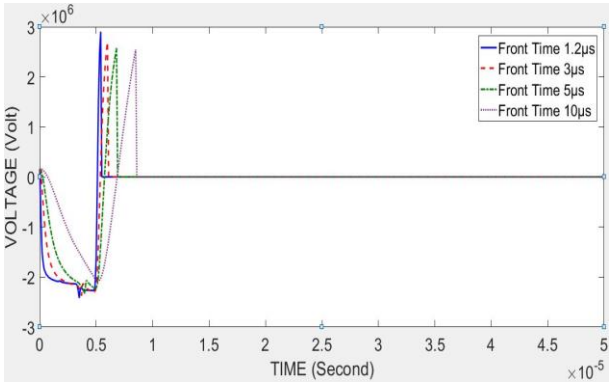

Fig. 13. Voltage across insulator holding phase C due to direct strike on overhead ground wire for different front times.

Table 1
Time to Flashover Occurrence Due To Direct Strike on the Overhead Ground Wire For Different Front Times

	Time to Flashover Occurrence			
	Front Time 1.2μs	***Front Time 3μs***	***Front Time 5μs***	***Front Time 10μs***
Insulator holding phase A	3.5μs	3.7μs	4μs	9.5μs
Insulator holding phase C	5.5μs	6μs	6.8μs	8.6μs

Similarly in the next case that is lightning strike on the tower top 100kA surge current of a fixed tail time has been injected for different front times of 1.2μs, 3μs, 5μs and 10μs. Fig. 14 and Fig. 15 illustrates the voltage wave shapes across the insulators holding phase A and phase C respectively. Table 2 shows the time to insulator flashover occurrence for different front times. For the insulator holding phase A flashover occurs only

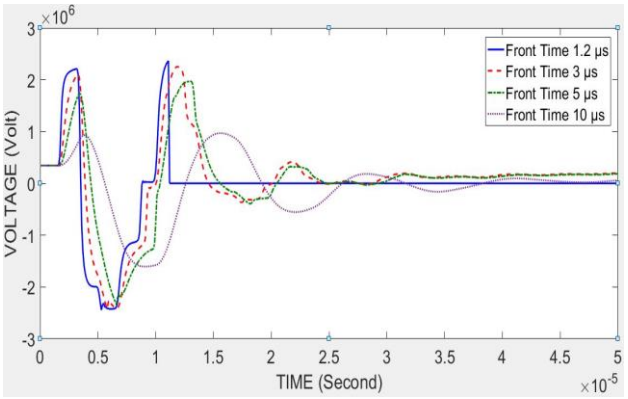

Fig. 14. Voltage across insulator holding phase A due to direct strike on tower top for different front times.

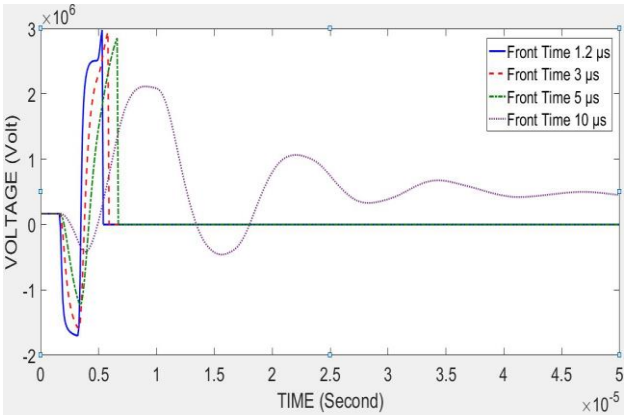

Fig.15. Voltage across insulator holding phase C due to direct strike on tower top for different front times.

Table 2
Time to Flashover Occurrence Due To Direct Strike on the Tower Top for Different Front Times

	Time to Flashover Occurrence			
	Front Time 1.2μs	***Front Time 3μs***	***Front Time 5μs***	***Front Time 10μs***
Insulator holding phase A	11.1μs	No Flash-over	No Flash-over	No Flash-over
Insulator holding phase C	5.3μs	5.8μs	6.6μs	No Flash-over

for the 1.2μs front time. But for higher front times the voltage across the insulator is not severe enough to intersect the volt-time characteristic curve and hence no flashover has been observed. In case of the insulator holding phase C, 1.2μs front time surge current causes the fastest flashover. Higher values of the front time take longer time for the insulator flashover to appear. The least severe case which contains the surge current of 10μs front time no flashover has been observed as the voltage shape

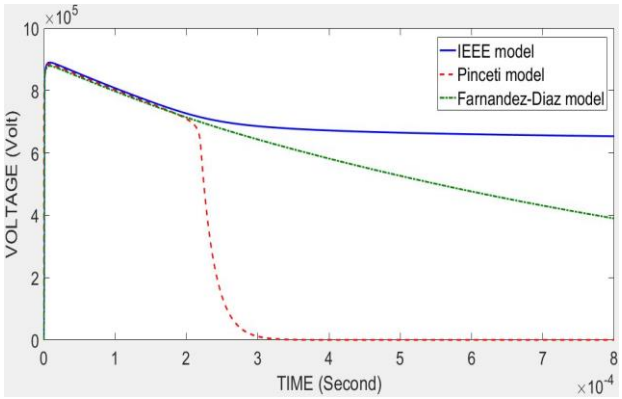

Fig.16. Residual voltage of 336kV ABB PEXLIM Q surge arrester for 20kA (8/20μs) surge current.

Table 3
Residual Voltage of 336 kV ABB PEXLIM Q Surge Arrester for 20kA (8/20μs) Surge Current

Surge Arrester Model	**Observed residual voltage in ATP Draw**	**Residual voltage in Data sheet**	**Difference (%)**
IEEE	889 kV	869 kV	2.3%
Pinceti	883 kV		1.6%
Fernandez-Diaz	879 kV		1.15%

between the insulators terminals could not intersect the volt-time characteristic curve.

In both cases, no flashover is observed across the insulator holding Phase B which is installed in the horizontally middle position of the tower.

3.2.3 Surge Arrester Performance

IEEE Pinceti and Farnandez-Diaz models for the selected surge arrester ABB PEXLIM Q with a rated voltage 336kV have been compared by injecting 20kA (8/20μs) surge current into each model in ATP Draw. The observed residual voltage for IEEE, Pinceti and Farnandez-Diaz Model were 889 kV, 883 kV and 879 kV shown in Fig. 16. According the manufacturer's datasheet residual voltage of the arrester for 20kA (8/20μs) is 869kV [23]. So from Table 3, it is apparent that the deviation from the manufacture provided data is less for Farnandez-Diaz model. Thus Farnandez-Diaz model shows better accuracy in this case. Lightning Surge has been considered to hit overhead ground wire. Induced overvoltage shape on the phase conductors is shown in Fig.17. The maximum overvoltage on phase conductor A, B and C is respectively 3.27 MV, 2.49MV and 2.56 MV respectively.

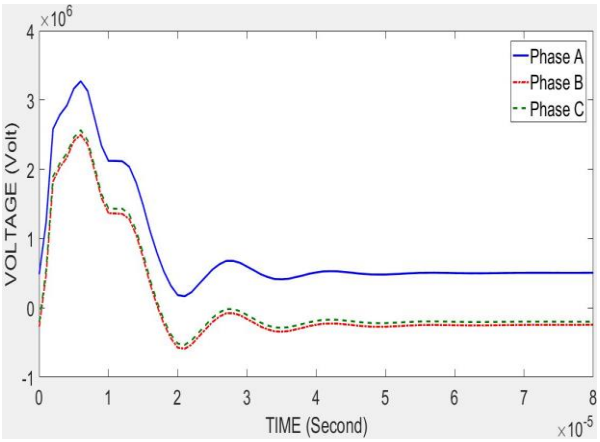

Fig.17. Induced overvoltage on the phase conductors due to direct strike on overhead ground wire.

Induced voltage with surge arresters on the phase conductors for this case is shown in Fig. 18. From Table 4, the maximum voltages with surge arresters on the phase conductors A, B and C are 0.824 MV, 0.816 MV and 0.816MV when the lightning strikes the Overhead Ground Wire. Basic Insulation Level (BIL) of the connected equipment and transformer a 400 kV transmission system is around. 1.55 MV [20]. Thus it is apparent that transmission line surge arresters have reduced the magnitude of the overvoltage induced on the phase conductors to a value below the Basic Insulation Level (BIL) preventing line outage.

In the next case surge current is injected onto the tower top. Induced voltage on the phase conductors is presented in Fig. 19. The observed peak value of the induced voltage of phases A, B and C conductors are 2.22 MV, 1.67 MV and 1.68 MV. Adding transmission line surge arresters has significantly reduced the phase conductors induced voltage which is shown in Fig. 20 and from Table 5 respectively on phase A, B and C peak induced voltages are 0.814 MV, 0.8 MV, 0.801MV.

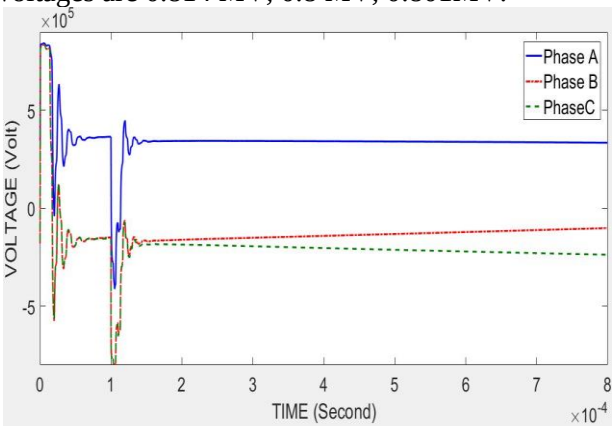

Fig.18. Induced overvoltage on the phase conductors due to direct strike on overhead ground wire with surge arrester.

Table 4
Maximum Voltage on Phase Conductors Due To Overhead Ground Wire Lightning Strike

Phase Conductor	Without Arrester	With Arrester	Over-voltage Suppression
A	3.27 MV	0.824 MV	74.8%
B	2.49 MV	0.816 MV	67.2%
C	2.56 MV	0.816 MV	68.1%

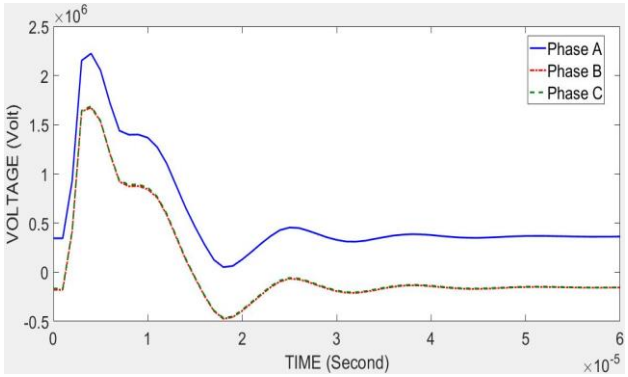

Fig.19. Induced overvoltage on the phase conductors due to direct strike on tower top.

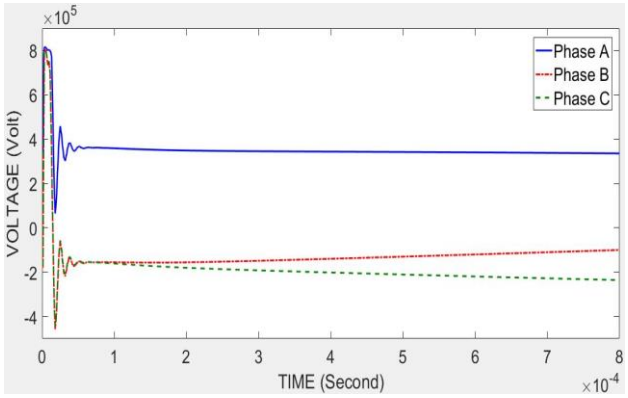

Fig.20. Induced overvoltage on the phase conductors due to direct strike on tower top with surge arrester.

Table 5
Maximum Voltage on Phase Conductors Due To Tower Top Lightning Strike

Phase Conductor	Without Arrester	With Arrester	Over-voltage Suppression
A	2.22 MV	0.814 MV	63.3%
B	1.67 MV	0.800 MV	52%
C	1.68 MV	0.801 MV	52.3%

Surge current has been imposed on the phase conductor in the next case to simulate the shielding failure event. Phase A conductor was considered to be hit directly by the lightning impulse current. The other phase conductors remain unaffected in this case. Waveforms of induced voltage on phase A conductor before and after applying surge arrester is

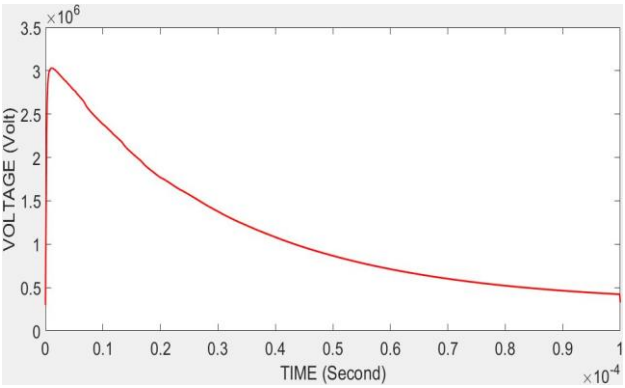

Fig.21. Induced overvoltage on the phase conductor A due to direct strike.

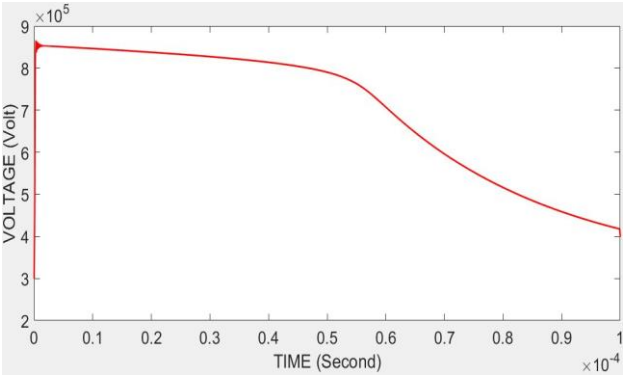

Fig.22. Induced overvoltage on the phase conductor A due to direct strike with surge arrester.

Table 6
Maximum Induced Voltage on Phase A Conductor Due To Direct Lightning Strike

Without arrester	With arrester	Over-voltage Suppression
3.01 MV	0.862 MV	71.3%

shown in Fig. 21 and Fig. 22. From Table 6 it is apparent that applying transmission line surge arresters reduced the maximum induced voltage from 3.01 MV to 0.862 MV on phase A conductor.

4 Conclusion

Lighting surge response of a 400kV transmission system has been analyzed in details using ATP/EMTP. According to the obtained results, it is apparent that front time of the lighting surge current has a great influence on the induced overvoltage and magnitude of the induced voltage is higher for the shorter front time. But varying the tail time does not significantly affect the peak induced voltage value. Insulator flashover simulation results present that reducing the front time of the surge current causes steeper overvoltage across the insulators thus lower the front time causes faster insulator flashover occurrence. From Insulator flashover simulation results it has also been observed that insulator strings at the two horizontal ends of the tower are more prone to flashover occurrence during lightning phenomenon. Thus this observation can be taken into account during tower structure design and transmission line and insulator string erection to reduce the damage to the insulator string during lightning surge phenomenon by preventing insulator flashover.

From the simulation results it has been observed that induced overvoltage on the transmission lines can be much higher than the suggested Basic Impulse Level which may cause line outage or severe damage to the connected equipment due to the travelling waves of severe magnitudes for each of the mentioned three case scenarios. Transmission line surge arresters have been implemented and it is observed that surge arresters reduce the induced overvoltage under the Basic Impulse Level thus preventing line outage and other equipment failure. A significant observation is that the percentage overvoltage suppression of the arrester is higher for greater induced voltage and in this study the range of the percentage overvoltage suppression is 52% to 74.8%. For the protection of electrical equipments and power outage from lightning induced overvoltage this research analysis will play a significant role.

References:

[1] M. Ishii, et al, "Multistory transmission tower model for lightning surge analysis", *IEEE Transaction on Power Delivery*, Vol. 6, No. 3, 1991, pp.1327-1335.

[2] T. Hara and O. Yamamoto, "Modeling of a transmission tower for lightning-surge analysis", *IEE Proc.-Gener, Transm. Distrib*, Vol. 143, No.3, 1996.

[3] M. S. Yusuf, M. Ahmad, M. A. Rashid, and M. O. Goni, "Analysis of Lightning Surge Characteristics on Transmission Tower", *Journal of Engineering Letters*, Vol. 23, No. 1, 2015, pp. 29-39.

[4] N. Zawania, Junainaha, Imrana and M Faizuhar, "Modelling of 132kV overhead transmission lines by using ATP/EMTP for shielding failure pattern recognition", *Procedia Engineering*, Vol. 53, 2013, pp.278 – 287.

[5] T. Ueda, T. Ito , H. Watanabe ,T. Funabashi and A. Ametani, "A comparison between two tower models for lightning surge analysis of 77 kV system", *PowerCon International Conference on Power System Technology Proceedings*, Perth, WA, Australia, 4-7 December, 2000.

[6] M. Kizilcay, C. Neumann, "Lightning overvoltage analysis of a 380-kV overhead line with a GIL section", *International Conference on Power Systems Transients (IPST)*, Cavtat, Croatia 15-17 June, 2015.

[7] S. Mohajeryami and M. Doostan, "Including surge arresters in lightning performance analysis of 132kV transmission tower", *IEEE/PES Transmission and Distribution Conference and Exposition (T&D)*, Dallas, TX, USA, 3-5 May, 2016.

[8] M. Qais and U. Khaled, " Evaluation of V-t characteristics caused by lighting strokes at different locations along transmission lines", *Journal of King Saud University - Engineering Sciences*, Vol. 30, No 2, , 2018, pp. 150-160.

[9] IEEE Working Group 3.4.11 "Modelling of metal oxide surge arrester", *IEEE Trans. On Power Delivery*, Vol.7, No 1, 1992, pp. 302-309.

[10] P. Pinceti and M. Giannettoni, "A simplified model for zinc oxide surge arresters", *IEEE Transactions on Power Delivery*, Vol. 14, No. 2, 1999, pp 393-398.

[11] F. Fernandez and R. Diaz, "Metal oxide surge arrester model for fast transient simulations". *International Conference on Power System Transients*, June, 2001.

[12] S. Bedoui, A. BayadiandA. M. Haddad, " Analysis of lightning protection with transmission line arrester using ATP/EMTP : case of an HV 220kV double circuit line", *45th International Universities Power Engineering Conference UPEC*, Cardiff, Wales, UK, 31 Aug.-3 Sept, 2010.

[13] M. Z. Islam, M. R. Rashed and M. S. Yusuf, "ATP-EMTP modelling and performance test of different type of lighting arrester on 132kV overhead transmission tower", *3rd International Conference on Electrical Information and Communication Technology (EICT)*, Khulna, Bangladesh, 7-9 December, 2017.

[14] EltrimaKable.a[Online].aAvailable:ahttps://www.eltrim.com.pl/wpcontent/uploads/2017/03/AFL-8.pdf.

[15] EltrimaKable.a[Online].aAvailable:ahttps://www.eltrim.com.pl/wpcontent/uploads/2017/03/AFL-17.pdf.

[16] J. A. Martinez-Velasco and Ferley Castro-Aranda, "Modelling of overhead transmission lines for lightning studies", *International Conference on Power Systems Transients (IPST)*, Montreal, Canada, 19-23 June, 2005.

[17] M. Łoboda and K. Lenarczyk, "Correlation between recorded CG lightningdischarges and shut-downs of selected HV overhead power transmission lines in Poland", *International Conference on Lightning Protection (ICLP)*, Shanghai, China, 2014.

[18] CIGRE Working Group 33-01, "Guide to procedures for estimating the lightning performance of transmission lines", *Technical Brochure*, October, 1991.

[19] IEEE Task Force on Fast Front Transients, "Modeling guidelines for fast transients*," IEEE Transaction on Power Delivery*, Vol. 11, No. 1, 1996, pp. 493–506.

[20] B. Oza, N. Nair, R. Mehta and V. Makwana, *Power system protection and switchgear*, New Delhi: Tata McGraw-Hill Education Private Ltd, 2010.

[21] F. Heidler, J.M.Cveti and B. V. Stani, "Calculation of Lightning Current Parameters", *IEEE Transaction on Power Delivery*,Vol. 14, No. 2, 1999, pp. 309-404.

[22] M. R. B. Tavakoli and B. Vahidi, "A Metamodeling Approach for Leader Progression Model-based Shielding Failure Rate Calculation of Transmission Lines Using Artificial Netural Network", *Journal of Electrical Engineering and Technology*, Vol: 6, No: 6, 2011, pp 760-768.

[23] Library.e.abb.com. (2008). [Online] Available at:https://library.e.abb.com/public/03d3975bfd1189dcc1257b130057b933/Surge%20Arrester%20Buyers%20Guide%20Edition%206%20-%20Section%20PEXLIM%20Q.pdf.